http://dx.doi.org/10.5935/0103-5053.20150092

J. Braz. Chem. Soc., Vol. 26, No. 6, 1265-1273, 2015.
Printed in Brazil - ©2015 Sociedade Brasileira de Química
0103 - 5053 $6.00+0.00

Article

Multiple Dynamics of Hydrazone Based Compounds

Elkin L. Romero,[a] Richard F. D'Vries,[b] Fabio Zuluaga[a] and Manuel N. Chaur[,a]*

[a]*Departamento de Química, Universidad del Valle, A.A., 25360 Cali, Colombia*

[b]*Instituto de Física de São Carlos, 13566-590 São Carlos-SP, Brazil*

Hydrazone derivatives of 2-quinolinecarboxaldehyde and 6-bromo-2-pyridinecarboxaldehyde were synthesized by sequence reactions with hydrazine derivatives. These compounds exhibited *E*/*Z* isomerization upon irradiation using a mercury lamp (250 W). The configurational changes were monitored by ^{1}H nuclear magnetic resonance (NMR), UV-Vis and fluorescence spectroscopy. Data of concentration of the *E*/*Z* isomers *versus* time showed first order kinetics with constants ranging from 0.024 to 0.0799 min^{-1}. The *Z* isomers were isolated by chromatographic methods and characterized by ^{1}H NMR, UV-Vis and fluorescence spectroscopy and X-ray diffraction. The *Z* compounds are stable even in solution for several months. Such stability is due to a thermodynamic stabilization by the formation of an intramolecular hydrogen bond in the *Z* structure, which is not seen in the *E* configuration. Furthermore, some of the compounds were used as ligands for various metal centers (Zn^{2+}, Co^{2+} and Hg^{2+}) and their electronic properties were studied including measurements of cyclic voltammetry. The compounds studied herein allow their use as dynamic systems in dynamic combinatorial chemistry as their properties can be modulated by light, heat and the presence of metal centers. Besides, obtaining a metastable state (*Z*-isomer) allows the use of these compounds as photo-brakes, and therefore they can be implemented as molecular machines.

Keywords: hydrazone compounds, configurational dynamics, photo-brakes, electrochemistry

Introduction

Molecular machines, systems designed to perform delicate and precise tasks, are remote from the original concepts of the dynamic combinatorial chemistry (DCC), but these systems share a characteristic from the dynamic combinatorial libraries (DCL) exploiting dynamic covalent bonds to steer the composition of systems by external physical/chemical stimuli and using these changes to extract information to perform work.[1] Currently, there has been a production of molecular systems whose physical and chemical properties can be reversibly modulated in response to an external stimulus, either light,[2–7] heat,[4,8] addition of metal ions,[9,10] pH changes[11-13] or electrochemical potentials.[14] These systems, also called "molecular switches"[15] are of great interest in the field of nanotechnology.[5]

The hydrazones have caught the attention for their use as molecular systems,[16-18] capable of undergoing reversible changes of configuration, *E/Z* isomerization,[4,16-21] which are favored by the presence of an additional nitrogen atom that diminishes the double-bond character of the ϖ system and facilitates isomerization;[22] *E/Z* isomerization could occur by either of two different mechanisms: rotation and inversion.

The former occurs through a polar transition state and results in the rotation of the substituents around the C=N double bond. The second mechanism occurs through inversion around the imine nitrogen and goes through a non-polar transition state.[12,16] However, more recent studies have demonstrated that azo-hydrazone tautomerism and rotation of the C–N bond is the most likely isomerization mechanism for systems involving an intramolecular hydrogen bond.[12] Moreover, the reversibility of the C=N bond, hydrazones can undergo constitutional changes leading to the formation of another useful compound.[4,16,17] These compounds may exhibit coordination dynamics by the presence of coordination sites in the chemical structure, this feature allows the locking and unlocking, controlled by metal ions, and therefore the reversible transformation of different states.[4,23,24]

The aforementioned properties of hydrazones have enabled them to be used in supramolecular chemistry[17] as molecular switches,[2,3] metallo-assemblies[19-21] and sensors[17,18] of both cations and anions. Likewise other systems including light driven molecular motors have been developed[2] and in that sense many of these systems can be implemented as

*e-mail: manuel.chaur@correounivalle.edu.co

digital molecular information storage systems due to the multiple dynamics that they exhibit in a reversible fashion.

Herein we studied the configurational dynamics of different hydrazone derivatives of 6-bromo-2-pyridinecarboxaldehyde and 2-quinolinecarboxaldehyde, which have been designed to show in the *Z* state, an intramolecular hydrogen bond formed between the amine hydrogen and the pyridine or quinoline ring nitrogen (Scheme 1) in order to stabilize the otherwise thermodynamically unstable *Z* isomer. Kinetics of the photoisomerization process was followed by ^{1}H nuclear magnetic resonance (NMR), UV-Vis and fluorescence spectroscopy. Additionally, these compounds were used as ligands to various metal centers (Zn^{2+}, Co^{2+} and Hg^{2+}) and their electronic properties were studied including measurements of cyclic voltammetry.

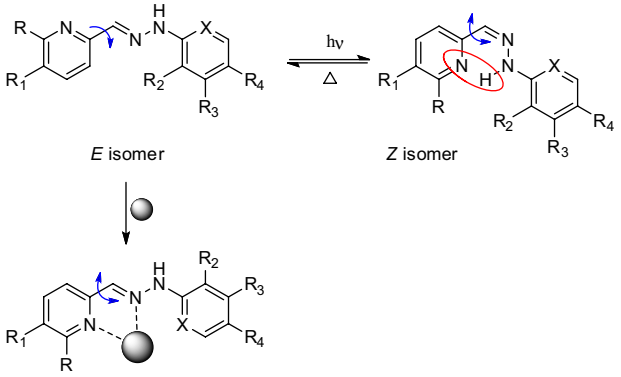

Scheme 1. Dynamic characteristics shown by the compounds studied: configuration change, E/Z isomerization and coordination with a metallic center.

Experimental

All starting reagents were acquired from Sigma-Aldrich and were used without additional purification. Infrared (IR) spectra were recorded on a Shimadzu FTIR 8400 spectrophotometer in KBr disks and films. NMR spectra (1D and 2D) were recorded on a 400 MHz Bruker Ultrashield spectrometer. UV-Vis and fluorescence spectra were taken in PharmaSpec Shimadzu UV-Vis UV-1700 spectrophotometer and Jasco FP-8500 spectrofluorimeter, respectively. Cyclic voltammograms were recorded in a bipotentiostat model 700 B series electrochemical Analyzer/Workstation from CHI Instruments coupled to a computer.

General procedure for oxidation lateral chains

A solution of the quinaldine (1.0 equiv.) and selenium dioxide (1.7 equiv.) in dioxane/water was heated under reflux monitored by thin-layer chromatography (TLC). The solid formed was filtered and washed with dichloromethane (2 × 2 mL). The filtrates were combined and the solvent removed under reduced pressure and the resulting oily residue was purified by column chromatography in dichloromethane.

General procedure for hydrazone synthesis

The hydrazine derivative (1.0 equiv.) was added to an ethanolic solution of the aldehyde (1.0 equiv.), subjected to reflux during 3 h. The precipitate was collected by vacuum filtration and washed with cold ethanol to obtain the pure product.

General procedure for hydrazone isomerization

Irradiations were carried out with a mercury lamp and samples were irradiated in NMR tubes; NMR, UV-Vis and fluorescence spectra were immediately recorded.

Results and Discussion

Synthesis of hydrazone precursors (**11a-b**)

The carbonyl compounds were obtained by oxidation of the corresponding 2-methylquinoline **10a-b** under reflux

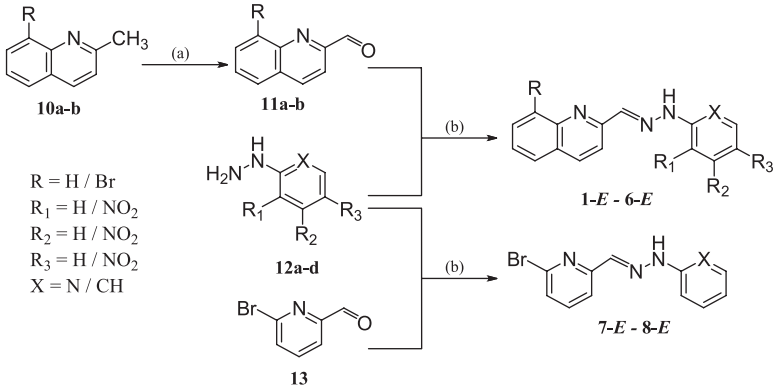

Scheme 2. Synthesis of hydrazonic derivatives **1-8.** (a) SeO_2/dioxane, reflux;[25] (b) ethanol/reflux.

using selenium dioxide in 1,4-dioxane and few drops of water (Scheme 2).[25] The reaction was monitored by TLC and purified by column chromatography using dichloromethane as eluent; the IR spectrum of compound **11a** taken in KBr pellet showed an absorption band at 1712 cm^{-1} corresponding to the stretching vibration of the carbonyl group. In the ^1H NMR spectrum of compound **11a** a singlet at 10.22 ppm corresponding to the aldehyde proton was observed. All types of carbon atoms were completely assigned 2D NMR techniques.

Synthesis of hydrazone compounds

The reaction of the synthesized carbonyl compounds, **11a**-**b** and **13**, with hydrazine derivatives **12a**-**d**, under ethanol reflux, led to the formation of the corresponding *E*-hydrazone compounds **1**-**8** (Scheme 2) with yields between 74 and 85%. The compounds were fully characterized by spectroscopic techniques such as IR and 1D and 2D NMR (see Supplementary Information (SI) section). The structural elucidation of the **8**-***E***[26] and **2**-***E*** compounds was confirmed by single crystal X-ray diffraction (Figure 1).

Crystals of compound **2**-***E*** were obtained by protonation of the hydrazonic derivative (**2**-***E***), as prismatic light red crystals, with monoclinic space group C2/c. In the asymmetric unit, one protonated hydrazone (**2**-***E***) molecule and one crystallographically independent chloride anion (Figure 1b) were observed. Each ionic pair forms dimeric subunits in which two chloride anions are shared between two organic molecules (Figure 2a) with distances N3–H3A···Cl1 = 3.022(2) Å and N1–H50···Cl1=3.180(2) Å. The dimeric subunits also forms pillars (supramolecular chains) by π-π stacking interactions with distances between centroids of 3.845(1) Å (Figure 2b) along the [1,1,0] and [–1,1,0] directions. The crystalline packing (Figure 2) is completed by weak C3-H3···π interactions with distances of 3.965(1) Å between each pillar.

On the other hand, the reported hydrazones exhibit high absorption coefficients in methanol, ε ca. 10^4 L mol^{-1} cm^{-1}, which is common for aromatic or heteroaromatic highly-conjugated systems in the UV region;[27-29] whereas, the data of electronic band gaps around 2.52-3.02 eV (Table 1) indicate that these compounds have highest occupied molecular orbital-lowest unoccupied molecular orbital (HOMO-LUMO) bands similar and the effect of the phenyl substituent does not exert a great influence on the relative energy of the molecular orbitals, however, it is only an estimate, an analysis more rigorous must include different substituents on both rings and solvent effects.[30]

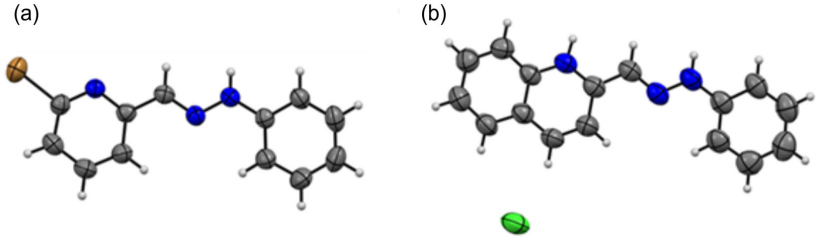

Figure 1. ORTEP drawing of (a) (*E*)-6-bromo-2-pyridine-carboxaldehyde-phenylhydrazone and (b) the asymmetric units of (*E*)-2-((2-(pyridin-2-yl) hydrazono)methyl)quinolin-1-ium chloride. Ellipsoids are displayed at the 50% probability level.

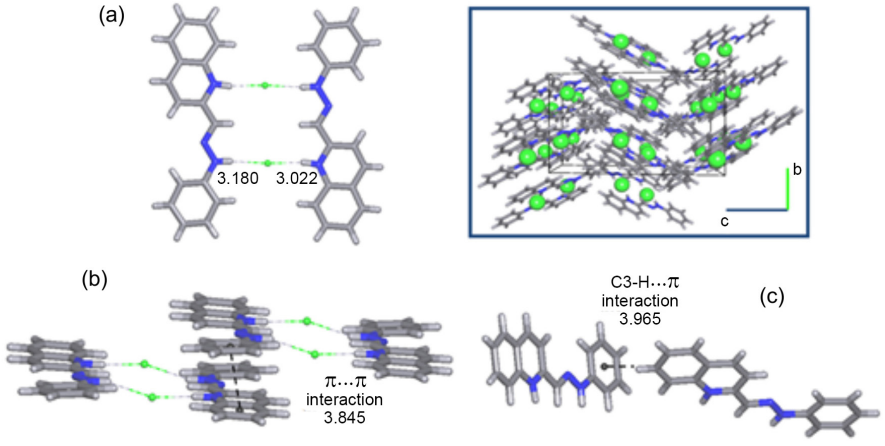

Figure 2. Representation of the (a) N–H···Cl, (b) π···π and (c) C–H···π supramolecular interactions for the compound **2**-***E*** (inset: [100] crystalline packing).

Table 1. Physical characteristics of the reported compounds

Compound	Aldehyde	Hydrazine	Yield / %	$\varepsilon \times 10^4$ / (L mol^{-1} cm^{-1})	ΔE_{elec} [a]
1-*E*	**11a**	**12a**	79	8.59	3.02
2-*E*	**11a**	**12b**	85	10.35	2.81
3-*E*	**11a**	**12c**	74	7.89	2.83
4-*E*	**11a**	**12d**	80	19.11	2.52
5-*E*	**11a**	**12e**	83	15.18	2.89
6-*E*	**11b**	**12a**	81	8.27	2.93
7-*E*	**13**	**12a**	85	13.66	2.97
8-*E*	**13**	**12b**	81	10.69	2.90

[a] ΔE_{elec} = 1240/Spectral onset (nm).

The results make them good candidates for their use in optical applications.

Response to photophysical stimulus (configurational dynamics)

Solutions of the hydrazone derivatives **1-*E*-6-*E*** in DMSO-d_6 were irradiated with a 250 W mercury lamp causing photochemical isomerization.[4,16] Configurational changes were monitored over time by ^{1}H NMR, UV-Vis and fluorescence spectroscopy. As observed in the ^{1}H NMR spectra shown in Figure 3, irradiation of the **1-*E*** solution in 450 µL of DMSO-d_6 and 50 µL of methanol during 100 min leads to the configurational transformation in **1-*Z*** with a 24% conversion when equilibrium is reached. This change occurs through a first order kinetics (k = 0.0328 min^{-1}). In comparison, photoisomerization of the herein reported quinoline compounds occur at a much slower rate. After ca. 60-75 min of irradiation some signals start to unfold, meaning a much slower isomerization rate. This behavior may be due to the substitution of the pyridine ring by the benzene ring, which reduces the acidity of hydrogen (*N*–H). Also, the presence of the bromide atom in the 8th position of the quinoline ring can produce an inductive effect decreasing the charge density of the quinoline nitrogen; as a consequence, the stabilization of the *Z* state is dismissed, which is reflected in the isomerization rate.

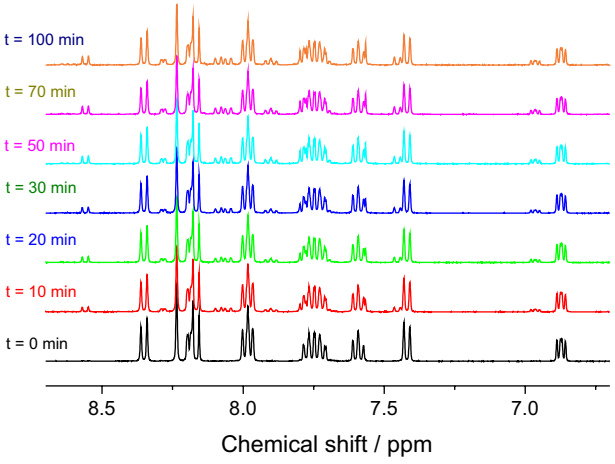

Figure 3. Expansion of the ^{1}H NMR spectrum (400 MHz) of a 41.3 mmol L^{-1} solution of **1-*E*** in DMSO-d_6 taken at different UV irradiation times.

Likewise, solutions of compounds **7-*E*** and **8-*E*** in CD_3OD were irradiated monitoring the changes by ^{1}H NMR spectroscopy. In this case, UV irradiation of **7-*E*** leads to the configurational isomerization towards **7-*Z*** in a 78% of conversion after a few minutes (Figure 4) thanks to the formation of an intramolecular hydrogen bond (Figure 4b) as it has been previously observed.[4] Photoisomerization was also conducted in DMSO-d_6, but in this case, isomerization occurs in a much lower rate, given that after 210 min of irradiation only 36% of the **7-*Z*** isomer was obtained, which clearly shows that photochemical induced isomerization depends on solvent polarity and the capacity of this for stabilizing the photo-induced transition state.[16]

Meanwhile, the isomerization rate of compound **8-*E*** is lower (k = 0.0183 min^{-1}) when compared to **7-*E*** (0.0799 min^{-1}), however, the yields of conversion allow the isolation of compound **8-*Z*** by column chromatography in 65% yield. The ^{1}H NMR spectrum of **8-*Z*** shows a high field displacement of the *N*–H proton due to the formation of the intramolecular hydrogen bond (Figure 3). On the other hand, the UV-Vis spectrum shows a hypsochromic shift (20 nm) in the main absorption peak (Figure 6); this shift is typical of n→π* transitions and it is caused by the formation of a intramolecular hydrogen bond, where the pyridine nitrogen donates its pair of electrons to the N–H proton, therefore, its n orbital energy level is decreased and the transition energy is increased, as a result, the absorbed photon energy is of shorter wavelength. The electronic HOMO-LUMO calculated by using the spectral onset, also reflects the lower bandgap of the *Z* state. Fluorescence is quenched in the *Z* state (Figure 6) due to a decrease in the conjugation of the molecule induced by the formation of

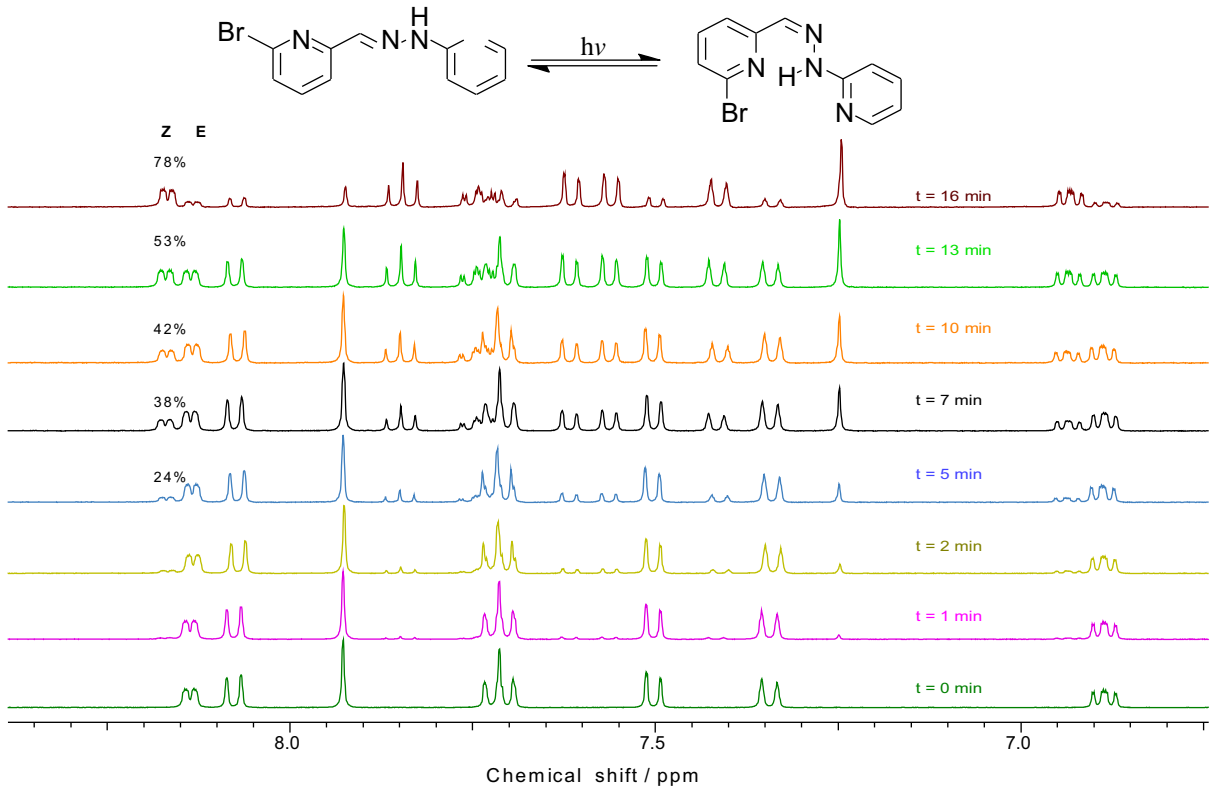

Figure 4. Expansion of the ^{1}H NMR spectrum (400 MHz) of a 48.3 mmol L^{-1} solution of **1**-***E*** in DMSO-d_6 taken at different UV irradiation times.

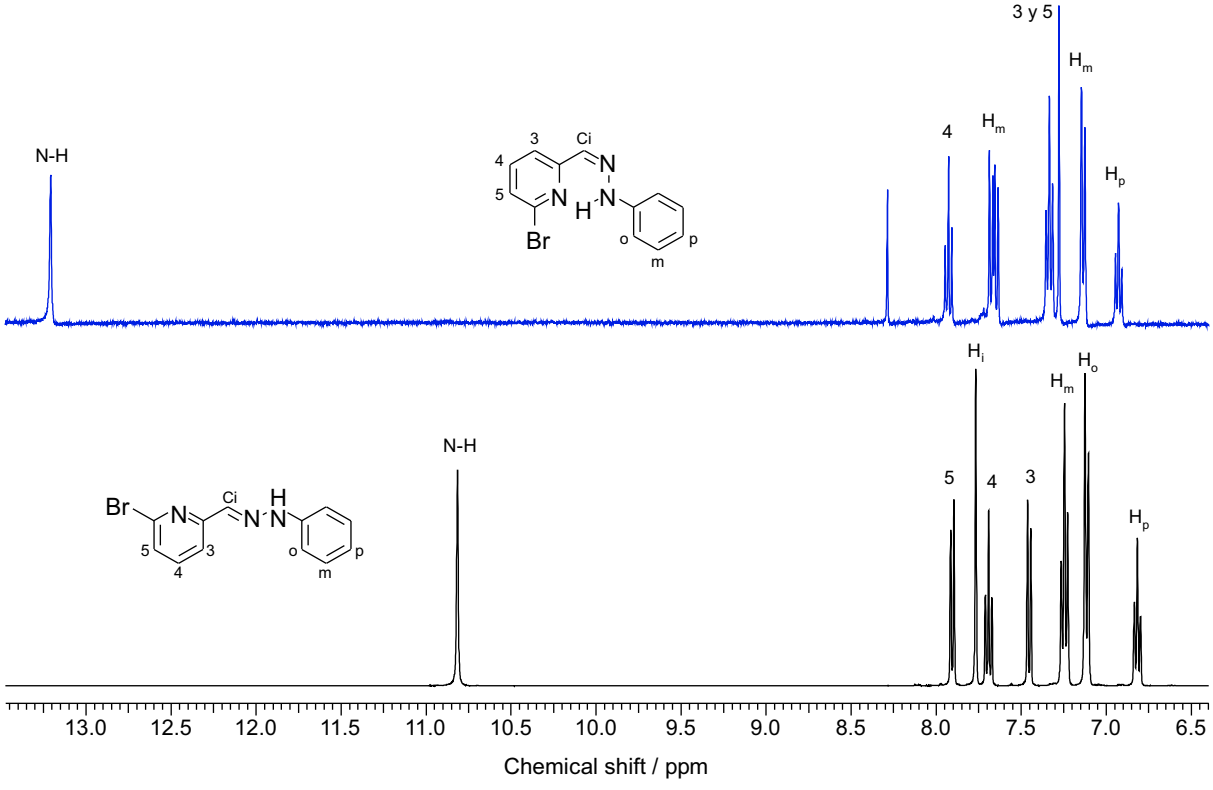

Figure 5. Expansion of the ^{1}H NMR spectrum (400 MHz) of **8**-***E*** and **8**-***Z*** in DMSO-d_6.

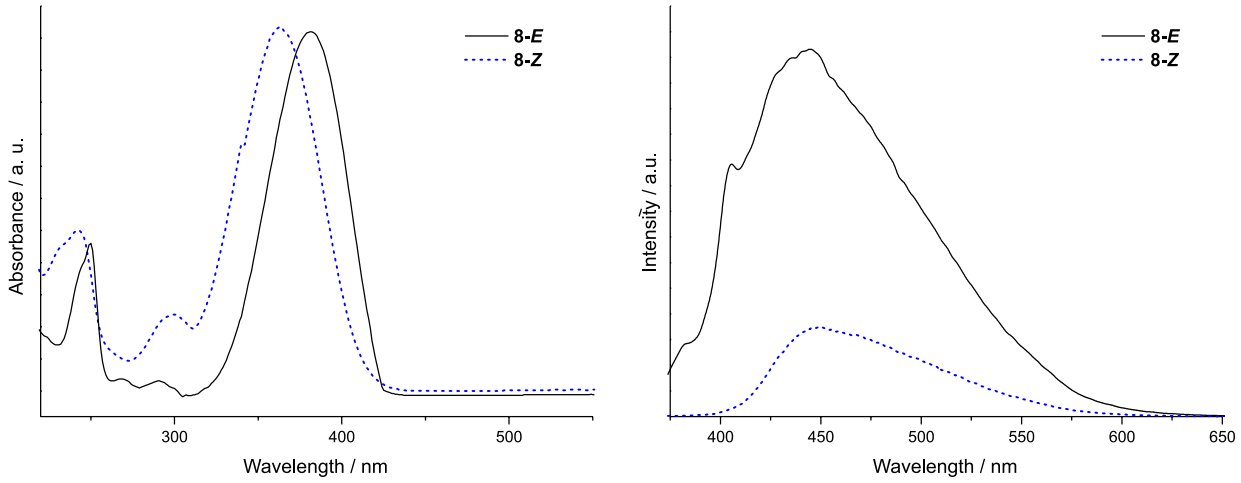

Figure 6. UV-Vis (left) and fluorescence (right) spectra of **8-*E*** and **8-*Z***. Excitation wavelength at 362 nm.

the hydrogen bond since the electron pair of the nitrogen of the pyridine ring is no longer part (at least in some extend) of the resonance at expense of the intramolecular hydrogen bond, which diminishes the conjugation in the framework and therefore decreases the wavelength absorption.[31]

Synthesis of hydrazone complexes

Complexes were obtained through the reaction of hydrazone compounds **7-*E*** and **8-*E*** with transition metal salts in +2 oxidation state (M^{2+}) in suitable solvents producing the precipitation of these compounds with yields between 59 and 82% (Table 2). These compounds were purified by washing with appropriated solvents and then they were characterized by FTIR and NMR spectroscopy and elemental analysis. When analyzing the proton NMR spectra of the metal complexes of compound **7-*E***, different displacements in some signals of the compound can be observed; the most marked is that for the *N*–H proton, which increases its displacement depending on the nature of the metal ion. As the formation of the metal complex proceeds, the N–*H* proton becomes unprotected displacing the signals by an inductive effect. Likewise, IR spectra show the characteristic bands for each hydrazone complex.

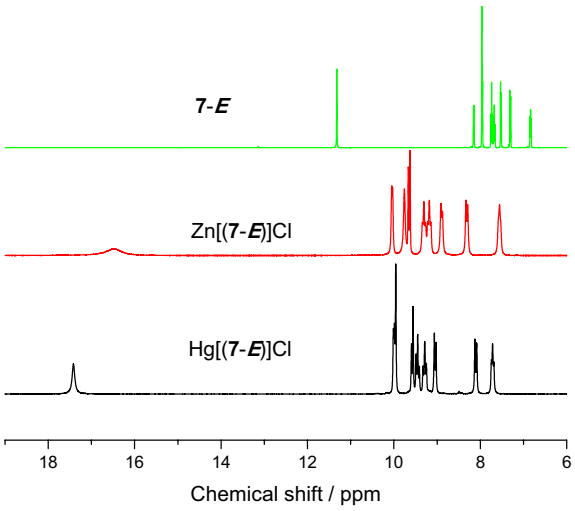

Figure 7. Expansion of the ^{1}H NMR spectrum (400 MHz) of hydrazone **7-*E*** and hydrazonic complexes M (**7-*E***) in DMSO-d_6.

Table 2. Characteristics of the hydrazone complexes

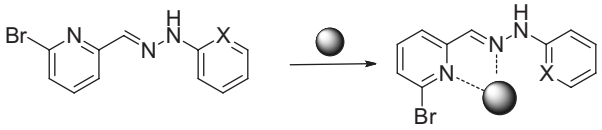

Compound	Hydrazone	Metallic salt	Yield / %	ε × 10^4 / (L mol^{-1} cm^{-1})	ΔE_{elec} [a]
9a	**7-*E***	$ZnCl_2$	69	6.87	2.77
9b	**7-*E***	$CoCl_2$	82	6.36	2.80
9c	**7-*E***	$HgCl_2$	71	9.50	2.74
9d	**8-*E***	$ZnCl_2$	59	6.29	2.59
9e	**8-*E***	$CoCl_2$	67	5.95	2.67
9f	**8-*E***	$HgCl_2$	76	7.96	2.63

[a]ΔE_{elec}= 1240/Spectral onset (nm).

UV-Vis spectra show a decrease in the maximum absorption band, which is accompanied by the appearance of new bands in the visible region corresponding to the absorption by metal ions, moreover, the spectral onsets (Table 2) reduce as the ionic radius increases, showing that the charge transfer interaction takes place within the molecule.[32] The emission spectrum shows, as expected, a drastic quenching of fluorescence by the addition of metal center, which promotes cross between systems, and diminishes the probability of fluorescence in as much as the coordination is carried out entirely by the unshared electrons of nitrogen, decreasing the contribution of these to the resonance of the system.

Response to pH changes of hydrazone complexes

The behavior of the hydrazone complexes was determined at different pH values and it was monitored through UV-Vis and fluorescence spectroscopies. For the cobalt complex **9b**, a displacement of the absorption bands is observed as well as an increase in the absorptivity coefficient and an increased fluorescence up to pH 8, due to a stronger interaction between the metal center and the deprotonated hydrogen of the amine (Figure 9).

Electrochemistry of the hydrazone complexes

In general, the metal complexes exhibit two irreversible oxidation and reductions steps, which depend on the nature of the metal, for example, the zinc(II) complex is oxidized more easily than its counterparts (see Table 3) due to its lower electronegativity, which facilitates the loss of an electron in the oxidative process.

Conclusions

The study of the chemical displacement of the hydrogen imine signal in NMR of the hydrazone as a function of

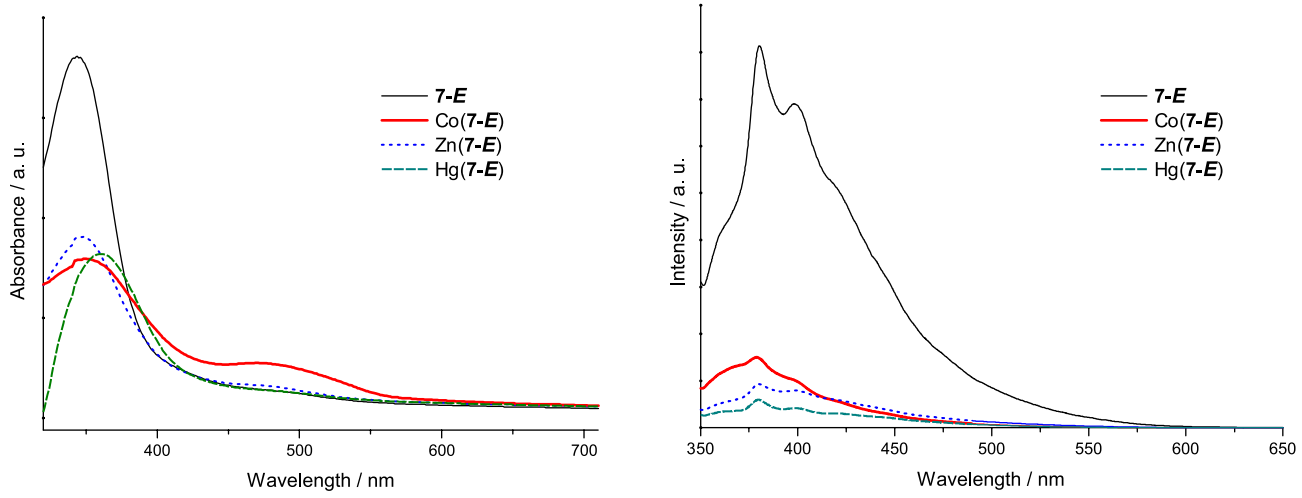

Figure 8. UV-Vis spectra (left) and fluorescence spectra (right) of hydrazone **7**-***E*** and hydrazone complexes M (**7**-***E***) in MeOH.

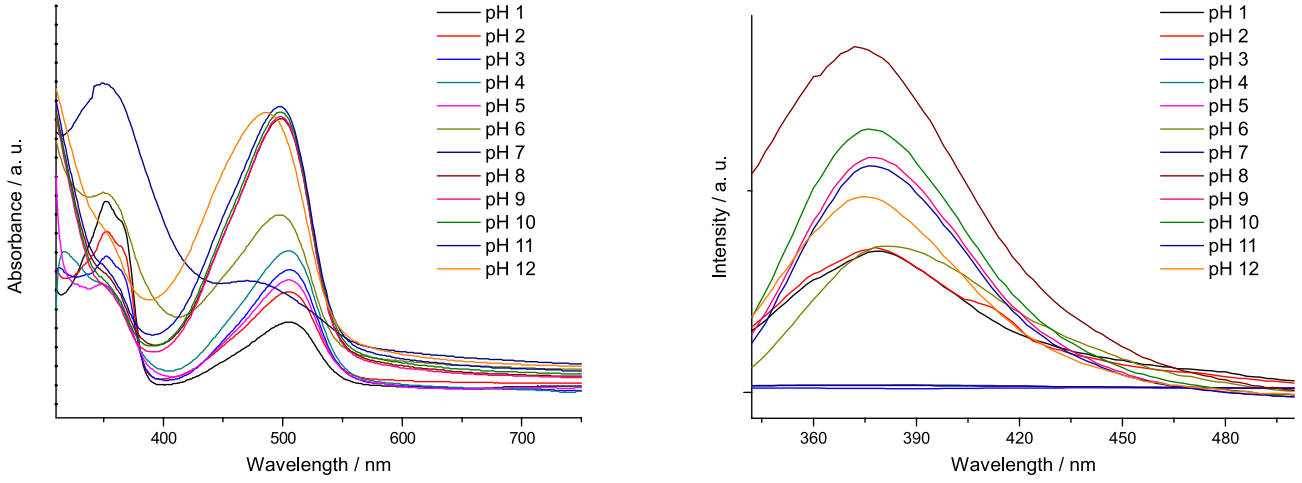

Figure 9. UV-Vis spectra (left) and fluorescence (right) of the [Co^{II}(**1**-***E***)] complex at different pH in MeOH.

Table 3. Oxidation / reduction potential [in V *vs.* (Fc^+/Fc)] of the hydrazone complexes obtained in THF + 0.1 mol L^{-1} $(n\text{-}Bu)_4NPF_6$

Compound	E_{ox2}	E_{ox1}	E_{red1}	E_{red2}	ΔE_{gap}	ΔE_{elec} [a]	X[b]
Zn(**7-*E***)]Cl_2	0.90	0.59	–	–	–	2.77	1.65
Co(**7-*E***)]Cl_2	0.97	0.73	–1.04	–1.97	1.74	2.80	1.88
Hg(**7-*E***)]Cl_2	1.00	0.64	–0.96	–	1.60	2.74	1.90

[a]ΔE_{elec}= 1240/SpectralOnset (nm); [b]Pauling electronegativity.[33]

the irradiation time reflects the obtention of a metastable system, which is thermodynamically stabilized due to the formation of an intramolecular hydrogen bond restricting the system's movement around the $C–C_{(imine)}$ and $N–C_{(hydrazine)}$ bonds, thus, functioning as a molecular motor in the *E* form and as a brake in the *Z* configuration. Likewise, movement of this bond is blocked by adding metal centers. The compounds prepared and studied herein corroborate the inherent dynamics of certain hydrazones toward physical and chemical stimulus and the results inspire the implementation of these systems in the design of molecular motors, photo-switches and cation sensors.

Supplementary Information

Supplementary data (full experimental details, ^1H and ^{13}C NMR, NMR spectra for all of the prepared compounds, and X-ray crystallographic data) are available free of charge at http://jbcs.sbq.org.br as PDF file.

Acknowledgements

The authors greatly thank the Vicerrectoría de Investigaciones of the Universidad del Valle, the Banco de la República, COLCIENCIAS and the Center of Excellence for Novel Materials (CENM) for the economic support to conduct this research. R. D. acknowledges a CAPES/PNPD scholarship from the Brazilian Ministry of Education and Crystallography group from IFSC-USP.

References

1. Li, J.; Nowak, P.; Otto, S.; *J. Am. Chem. Soc.* **2013**, *135*, 9222.
2. Cnossen, A.; Browne, W. R.; Feringa, B. L.; *Molecular Machines and Motors: Unidirectional Light-Driven Molecular Motors Based on Overcrowded Alkenes;* Springer-Verlag: Berlin, 2014.
3. Yamamura, S.; Tamaki, T.; Seki, T.; Sakuragi, M.; Kawanishi, Y.; Ichimura, K.; *Chem. Lett*. **1992**, 543.
4. Chaur, M. N.; Collado, D.; Lehn, J.-M.; *Chem. Eur. J.* **2011**, *17*, 248.
5. Hirose, K.; *J. Inclusion Phenom. Macrocyclic Chem.* **2010**, *68*, 1.
6. Kay, E. R.; Leigh, D.; Zerbetto, F.; *Angew. Chem., Int. Ed. Engl.* **2007**, *46*, 72.
7. Sun, W.-T.; Huang, S.-L.; Yao, H.-H.; Chen, I.-C.; Lin, Y.-C.; Yang, J. S.; *Org. Lett.* **2012**, *14*, 4154.
8. Coskun, A.; Friedman, D. C.; Li, H.; Patel, K.; Khatib, H.; Stoddart, J. F.; *J. Am. Chem. Soc.* **2009**, *131*, 2493.
9. Kelly, T. R.; Bowyer, M. C.; Bhaskar, K. V.; Bebbington, D.; García, A.; Lang, F.; Kim, M. H.; Jette, M. P.; *J. Am. Chem. Soc.* **1994**, *116*, 3657.
10. Ray, D.; Foy, J. T.; Hughes, R. P.; Aprahamian, I.; *Nat. Chem.* **2012**, *4*, 757.
11. Landge, S. M.; Tkatchouk, E.; Benítez, D.; Lanfranchi, D. A.; Elhabiri, M.; Goddard, W.; Aprahamian, I.; *J. Am. Chem. Soc.* **2011**, *133*, 9812.
12. Landge, S. M.; Aprahamian, I.; *J. Am. Chem. Soc.* **2009**, *131*, 18269.
13. Su, X.; Voskian, S.; Hughes, R. P.; Aprahamian, I.; *Angew. Chem., Int. Ed.* **2013**, *52*, 10734.
14. Yang, C.-H.; Prabhakar, C.; Huang, S.-L.; Lin, Y.-C.; Tan, W. S.; Misra, N. C.; Sun, W.-T.; Yang, J.-S.; *Org. Lett*. **2011**, *13*, 5632.
15. Balzani, V.; Credi, A.; Venturi, M.; *Molecular-Scale Machines*; Wiley-VCH: Veinheim, 2003.
16. Lehn, J.-M.; *Chem. Eur. J.* **2006**, *12*, 5910.
17. Su, X.; Aprahamian, I.; *Chem. Soc. Rev.* **2014**, *43*, 1963.
18. Tatum, L.; Su, X.; Aprahamian, I.; *Acc. Chem. Res.* **2014**, *47*, 2141.
19. Lehn, J. M.; Ulrich, S.; *J. Am. Chem. Soc*. **2009**, *131*, 5546.
20. Ruben, M.; Lehn, J-M.; Müller, P.; *Chem. Soc. Rev*. **2006**, *35*, 1056.
21. Hardy, J. G.; *Chem. Soc. Rev*. **2013**, *42*, 7881.
22. Dugave, C.; Demange, L.; *Chem. Rev.* **2003**, *103*, 2475.
23. Foy, J. T.; Ray, D.; Aprahamian, I.; *Chem. Sci.* **2015**, *6*, 209.
24. Su, X.; Robbins, T. F.; Aprahamian, I.; *Angew. Chem., Int. Ed.* **2011**, *50*, 1841.
25. Deeming, A. J.; Rothwell, I. P.; Hursthouse, M. B.; Malik, K. M.; *J. Chem. Soc., Dalton Trans.* **1979**, 1899.
26. Moreno-Fuquen, R.; Chaur, M. N.; Romero, E. L.; Zuluaga, F.; Ellena, J.; *Acta Crystallogr.* **2012**, *E68*, o2131.
27. Sabbatini, N.; Guardigli, M.; Lehn, J. M.; *Coord. Chem. Rev.* **1993**, *123*, 201.

28. Montalti, M.; Credi, A.; Prodi, L.; Gandolfi, M. T.; *Handbook of Photochemistry*, 3rd ed.; CRC Press, Taylor & Francis: Boca Raton, 2006.
29. Armelao, L.; Quici, S.; Barigelletti, F.; Accorsi, G.; Bottaro, G.; Cavazzini, M.; Tondello, E.; *Coord. Chem. Rev.* **2010**, *254*, 487.
30. Prabavathi, N.; Nilufer, A.; Krishnakumar, V.; *Spectrochim. Acta, Part A* **2012**, *99*, 292.
31. Albani, J. R.; *Structure and Dynamics of Macromolecules: Absorption and Fluorescence Studies*, 1st ed.; Elsevier: London, 2004.
32. Nakamoto, K.; *Infrared and Raman Spectra of Inorganic and Coordination Compounds*, 4th ed.; John Wiley & Sons: New York, 1986.
33. Kaye, G. W. C.; Laby, T. H.; *Tables of Physical and Chemical Constants*, 16th ed.; Longman: London, 1995.

Submitted: January 27, 2015
Published online: April 17, 2015

FAPESP has sponsored the publication of this article.